Paramagnetic excitations in singlet ground state $PrNi_2Si_2$

J. A. Blanco
Departamento de Física, Universidad de Oviedo, 33007 Oviedo, Spain

R. M. Nicklow
Solid State Division, Oak Ridge National Laboratory, Oak Ridge, Tennessee 37831

D. Schmitt
Laboratoire Louis Néel, Centre National de la Recherche Scientifique, BP 166X, 38042, Grenoble, France

(Received 15 November 1996; revised manuscript received 30 May 1997)

The dispersion curves for magnetic excitations along the principal directions of the Brillouin zone of the singlet ground state compound $PrNi_2Si_2$ have been measured at 30 K by inelastic neutron-scattering experiments in the paramagnetic phase. From these data we have extracted information about the main exchange interaction coupling parameters J_{ij} that are responsible for the appearance of an amplitude modulated magnetic order in this compound below $T_N = 20$ K. The results are consistent with the long-range character of Ruderman-Kittel-Kasuya-Yosida interactions because in order to describe the dispersion curves observed at 30 K it is necessary to consider the influence of the interaction to the eighth nearest-neighbor Pr^{3+} ion along the c direction. In addition, we have studied the thermal dependence of the excitations at several representative points in the Brillouin zone that show an important softening as the temperature is lowered to T_N. [S0163-1829(97)03042-7]

I. INTRODUCTION

During the last few years several theoretical and experimental studies have been devoted[1–4] to the properties of incommensurate solids. Some of the well-known examples of these types of solids are electrons in a crystal subjected to an external magnetic field, incommensurate crystalline structures, and magnetic materials with an amplitude modulated (AM) arrangement of the moments. In the latter example, a large effort has been dedicated to the understanding of the magnetic excitations in such materials using different mathematical techniques, although, due to the finite character of the experimental resolution, some of the more detailed aspects of incommensurability have only a purely mathematical interest.

A large number of rare-earth intermetallic alloys have been found to exhibit AM ordering, at least in a limited temperature range. This type of ordering is believed to be a consequence of the frustration of competing interactions due to the long-range and oscillatory nature of the indirect exchange interactions of Ruderman-Kittel-Kasuya-Yosida (RKKY) type and to the existence of a large uniaxial anisotropy.[5] At low temperature, in most of these compounds, multistep metamagnetism could be observed as a consequence of the squaring up of a sinusoidal AM structure in an applied field; the system undergoes several magnetic transitions between the zero-field structure and the field induced ferromagnetic arrangement. Under the application of a magnetic field, the AM systems are generally characterized by a smooth metamagnetic behavior that corresponds to the progressive vanishing of the modulation.

One of the first examples of a longitudinally modulated incommensurate spin structure is Er metal, in which the spins order parallel to the c axis of the hcp crystalline structure. The transverse fluctuations in the AM structure of Er, which appears between $T_N = 84$ K and 52 K, show a broad energy distribution of neutron scattering owing to the spatial variations of the exchange and anisotropy energies, while the longitudinal fluctuations display rather sharp peaks that have a linear dispersion relation.[6] Several attempts were made in order to account for the magnetic excitations of Er metal, without complete success.[7] However, it has been recently shown that the experimental results in the ordered phase are in substantial agreement with the calculations obtained using a random-phase-approximation (RPA) theory that involves a N-sites diagonalization of the molecular-field Hamiltonian.[8] Nevertheless, there are still two significant inconsistencies: one above T_N, because some of the calculated excitations are not observed; and the other below T_N, where RPA does not account for the quasielastic signal detected for both the transverse and the longitudinal excitations.

The $PrNi_2Si_2$ compound is particularly interesting because it possesses an AM structure that is stable below $T_N = 20$ K down to 0 K,[9] owing to the existence of a nonmagnetic singlet state as the crystal-field ground state. In $PrNi_2Si_2$ the magnetic moments are also parallel to the c axis, as in the Er metal, with a propagation vector $Q = (0,0,0.875)$ in reduced units. For this reason this compound is a good candidate to study the magnetic excitations in AM systems over a large temperature range. In order to achieve this objective it is necessary to determine the crystalline electric field (CEF) and exchange coupling parameters which govern the magnetic behavior of the system below T_N. The CEF as well as the exchange parameters $J(0)$ and $J(Q)$ have been obtained from a complete joint analysis of different physical properties of $PrNi_2Si_2$. In fact, the CEF level scheme leads to a nonmagnetic ground state well isolated from the other levels, a second singlet and a magnetic doublet as the first two ex-

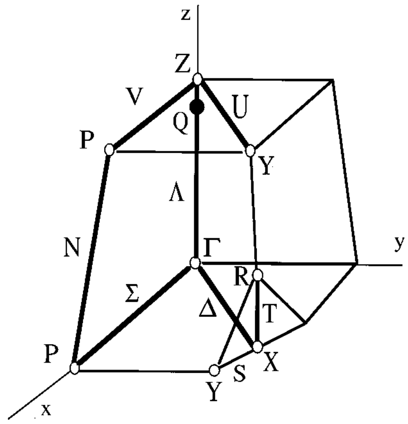

FIG. 1. Brillouin zone for a body-centered tetragonal lattice indicating the different directions investigated in this research.

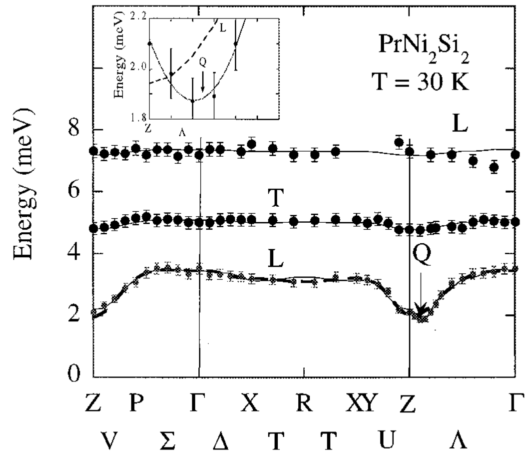

FIG. 2. Dispersion curves of the paramagnetic excitations in $PrNi_2Si_2$ at 30 K. The inset shows the detail of the minimum around Q. The solid line is calculated from the best fit (8 NN+5 NN, see below) of the lowest longitudinal L mode, while the dashed lines correspond to that in which only the 9 nearest-neighbor ions are considered at 30 K.

cited levels (see below), thereby explaining the persistence of the AM arrangement over the whole ordered temperature range.

The aim of this study is then to present a quantitative analysis of the dispersion curves obtained from inelastic neutron-scattering (INS) measurements at 30 K along the main directions of the Brillouin zone using the RPA theory described in detail in Ref. 10, as well as to analyze also the thermal dependence of the excitations at some representative points of the Brillouin zone between 30 K and T_N. This paper will complete some preliminary results of this work published elsewhere[10] and the main information we obtain will be used in the future to explain the magnetic excitations in the AM phase.

II. EXPERIMENTAL DETAILS

A single crystal of $PrNi_2Si_2$ of approximately 1 cm^3 was prepared using the Czochralski method at the Laboratoire Louis Néel. The purity of the crystal used in the present experiments is comparable to that of the crystal previously investigated by us in Ref. 9 ($a=b=4.047$ Å and $c=9.621$ Å). Most of the INS experiments reported here were carried out at 30 K at the Oak Ridge National Laboratory (ORNL) and were performed on the HB2 and HB3 triple-axis spectrometers located at the high-flux-isotope reactor. Data were collected for several scattering wave vector k along the main directions of the Brillouin zone (see Fig. 1) both parallel and perpendicular to the c axis in the (010) and (-110) planes. The INS measurements below 30 K (down to $T_N=20$ K) were carried out at the Institute Laue-Langevin of Grenoble on IN 12.

At ORNL the monochromator and analyzer were the (002) planes of pyrolytic graphite. In order to maintain optimum focusing conditions because the incoming neutron energy is changed during each scan, all the measurements were constant k scans with the scattered neutron energy fixed at 13.5 and 6.5 meV and with different collimations in order to produce energy resolutions [half width at half maximum (HWHM)] of about 0.5 and 0.25 meV, respectively. A PG filter was placed in the scattered beam in order to reduce possible spurius signals from harmonic wavelength contamination.

The results obtained in both experiments were then convoluted with a normalized Gaussian, the width of which was adjusted to give the best agreement with the experimental results.

III. EXPERIMENTAL RESULTS

The dispersion curves of the paramagnetic excitations in $PrNi_2Si_2$ at $T=30$ K are shown in Fig. 2 along the symmetry directions of the Brillouin zone that are depicted in Fig. 1. Three branches were observed over the measured energy range 1–9 meV. Two of them, those around 5 and 7.5 meV, are almost k-independent and are mainly related to transverse and to longitudinal excitations, respectively, (see below). However, the lowest energy branch, corresponding to a longitudinal excitation, has a well-defined dispersive character in the range 1.8–3.5 meV, and it is already very dispersive 10 K above T_N. Moreover, the vector $k=Q$ for which the $\omega(k)$ is minimum corresponds to the propagation vector of the AM structure stabilized below T_N.

Typical scans of these excitations at 30 K are represented in Fig. 3. Particular attention was paid to the spectra at the vectors associated with the Γ, Z, and Q points. It is worth noting that although Z and Q are quite close to each other, the variation of $\omega(k)$ in the vicinity of these points is quite important. Furthermore, the data of Fig. 3 clearly confirms the longitudinal or transverse nature of each of the observed branches as commented before in reference to Fig. 2. In fact, since the low-energy peaks are found only for the scattering vector k perpendicular to c^*, these excitations must be longitudinal. The measurements for the low-energy peaks near Z were made with neutrons of energy of 6.5 meV in order to give an energy resolution of about 0.25 meV HWHM. On the other hand, the high-energy peaks are seen for k both parallel and perpendicular to c^*. The intensity of the peak at an energy transfer of ~ 5 meV is much stronger in the scan at $k \| c^*$. By contrast, the intensity associated with the 7.5 meV branch has appreciable value only for $k \perp c^*$ as is observed at

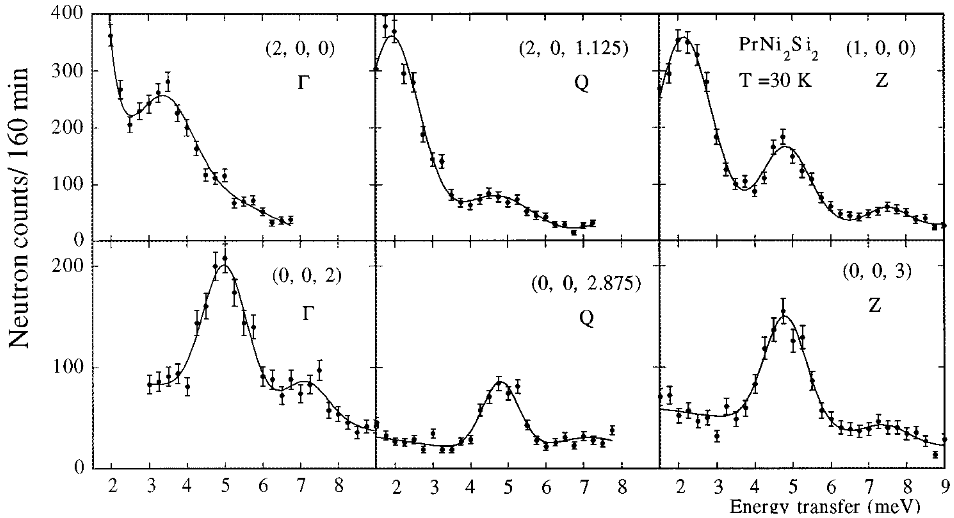

FIG. 3. Constant k scans of the $PrNi_2Si_2$ compound at 30 K for several k points (Γ, Z, and Q); the lines are least-squares fits.

(100) and it has an almost negligible value for k along c^*, indicating that the longitudinal contribution is the most important at 30 K. However, the data collected at 60 K (see Fig. 4) clearly shows that both longitudinal and transverse excitations are positioned at the same energies as for 30 K and have similar intensities at this higher temperature.

These features are in good agreement with the information obtained from a previous INS experiment on a powder sample that allowed us to determine the CEF level scheme of $PrNi_2Si_2$.[9] Figure 5 represents the CEF low-energy levels of this compound. This schematic picture could be used to identify the different branches observed in the present experiment. The lowest energy transfer corresponds to a longitudinal excitation from the singlet ground state Γ_1 to the first excited level Γ_2, by means of J_z. The transverse excitation centered at 5 meV is associated with a transition from the ground state to the second excited level, a doublet, $\Gamma_5^{(1)}$ by $J\pm$. Lastly, the excitation detected around 7.5 meV is related in principle to two possible transitions: one between the first excited level Γ_2 and the fourth excited level $\Gamma_1^{(2)}(L)$, and other between $\Gamma_1^{(2)}$ and $\Gamma_5^{(2)}$ levels (T). Nevertheless, some puzzling results are not well understood; the weak transverse excitation around 7.5 meV found at 30 K ($\Gamma_1^{(2)} \rightarrow \Gamma_5^{(2)}$) should be almost zero intensity at this temperature due to the thermal population factor. However, it is detected in the spectra of Fig. 3. On the other hand, in spite of this fact, the ratio of intensities between the transverse and longitudinal excitations at 60 K (see Fig. 4) is in good agreement with the calculations obtained using the CEF param-

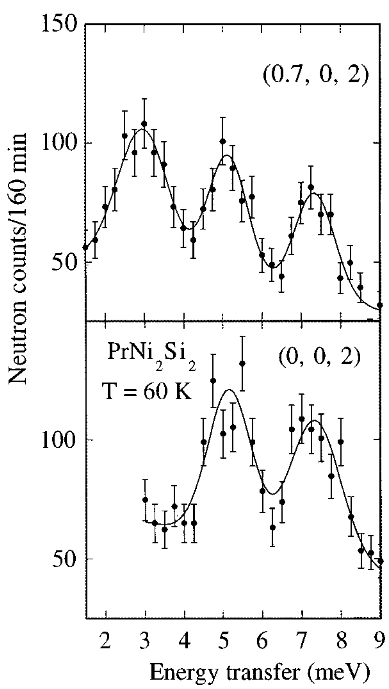

FIG. 4. Constant k scans of the $PrNi_2Si_2$ compound at 60 K for (0.7, 0, 2) and (0, 0, 2); solid lines are least-squares fits.

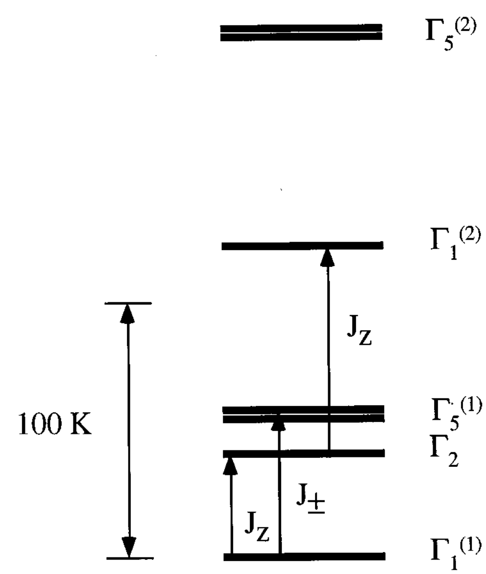

FIG. 5. Low-energy paramagnetic CEF level scheme of $PrNi_2Si_2$; arrows shows the main transitions observed by a powder INS experiment around 3, 5 and 7.5 meV and J_α ($\alpha = z$, + and −) indicates the matrix element which connects both states.

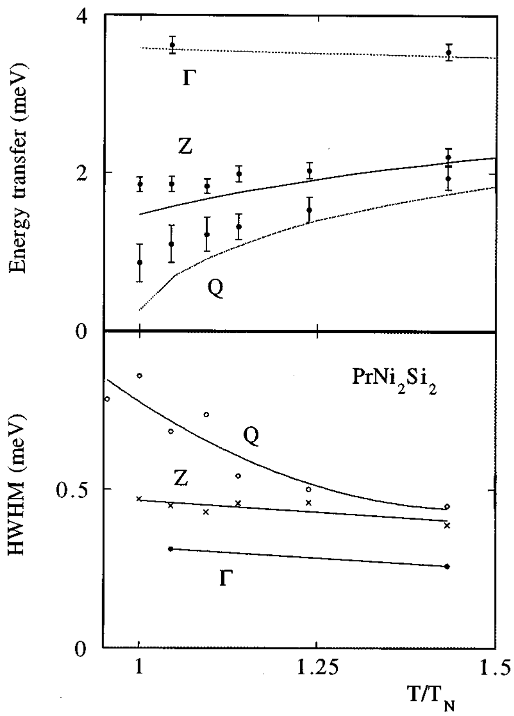

FIG. 6. Upper part: thermal dependence of $\omega(k)$ for Γ, Q, and Z. Solid lines are calculations using the J_{ij} parameters obtained from the least-squares procedure (see text). Lower part: thermal dependence of HWHM for these transfers showing the change of nature from inelastic to quasielastic type at Q when the temperature decreases. The lines are only guides for the eyes.

eters of Ref. 9, showing that both types of excitations are present.

In order to extend the information obtained at 30 K in the experiment at ORNL we have investigated the thermal dependence of the dispersion curves $\omega(k)$ at Γ, Q, and Z to see if there is (or not) a soft mode at these points. The thermal dependence of $\omega(k)$ is depicted in Fig. 6. The energy at Γ is almost temperature-independent, while for Q and Z, their values decrease when the temperature decreases; the variation of $\omega(k)$ at Q being larger than that at Z between 30 K and T_N, since the softening reaches about 50%. However, neither excitation corresponds to the case of a complete soft mode. An important difference between these two modes is the behavior of their energy widths γ=HWHM (see lower part of Fig. 6). At 30 K both γ are large, have only an inelastic character (at IN 12 the elastic peak has a γ of 0.2 meV) and they are quite similar in magnitude. But close to T_N the behavior of $\omega(Q)$ suggests a strong critical behavior; $\omega(Q)$ becomes quite small and quite large, being around 0.9 at 20 K as reflected in Fig. 7.

IV. THE RPA FORMALISM

Our starting point is the simplest model used to describe the occurrence of most of the observed properties in rare-earth magnetism. For the case of tetragonal symmetry, the Hamiltonian could be written as

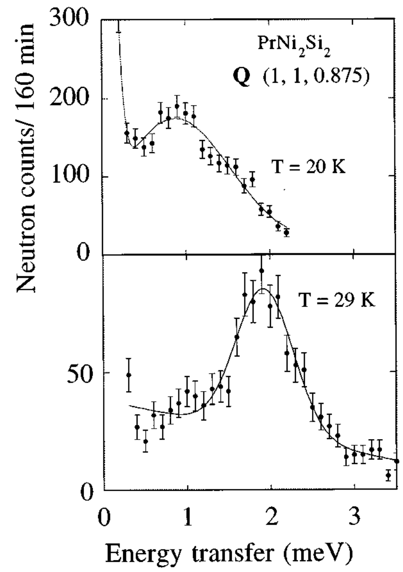

FIG. 7. Constant k scans of the PrNi$_2$Si$_2$ compound for Q at 29 and 20 K.

$$H=\sum_i B_2^0O_2^0(i)+B_4^0O_4^0(i)+B_4^4O_4^4(i)+B_6^0O_6^0(i)+B_6^4O_6^4(i)$$

$$-\sum_{i>j} J_{ij}\mathbf{J}_i\cdot\mathbf{J}_j\,. \tag{1}$$

The first term represents the single-ion CEF interaction involving the Stevens operators O_l^m, whereas the second one corresponds to the RKKY indirect exchange interactions. In order to determine the spectrum of the paramagnetic excitations, the formalism of the generalized susceptibilities $G^{\alpha\beta}(i,j,t)$ $(\alpha,\beta=z,+,-)$ can be introduced,[11] since the poles of their Fourier transform $G^{\alpha\beta}(\mathbf{q},\omega)$ give rise to the energy spectrum. Solving the equation of motion for these functions within the RPA theory leads to a linear system of coupled equations

$$\begin{aligned}G^{\alpha\beta}(\mathbf{q},\omega)=&g^{\alpha\beta}(\omega)-J(\mathbf{q})g^{\alpha z}(\omega)G^{z\beta}(\mathbf{q},\omega)\\&-\tfrac{1}{2}J(\mathbf{q})(g^{\alpha+}(\omega)G^{-\beta}(\mathbf{q},\omega)\\&+g^{\alpha-}(\omega)G^{+\beta}(\mathbf{q},\omega)),\end{aligned} \tag{2}$$

where the single-ion CEF susceptibilities are given by

$$g^{\alpha\beta}(\omega)=\sum_{m,n}\frac{\langle m|J_\alpha|n\rangle\langle n|J_\beta|m\rangle}{\omega-\omega_n+\omega_m}(f_m\text{-}f_n)$$

with f_m and f_n the thermal population factors of the CEF states $|m\rangle$ and $|n\rangle$, respectively, and $J(\mathbf{q})=\sum_{j\neq i}J_{ij}e^{i\mathbf{q}(\mathbf{R}_i-\mathbf{R}_j)}$ is the Fourier transform of the intersite exchange coupling constants J_{ij}.

The solution of the linear system (2) requires to a decoupling of the different excitation modes by using symmetry rules for the matrix elements which appears in $g^{\alpha\beta}(\omega)$. Generally, longitudinal and transverse excitations can be separated, corresponding, respectively, to $g^{zz}(\omega)$, $g^{+-}(\omega)$, and $g^{-+}(\omega)$. These selection rules arise because one can choose the axes of the coordinate system so that the expressions for the eigenfunctions have several vanishing components, leading to the following equations:

$$G^{zz}(\mathbf{q},\omega)=g^{zz}(\omega)-J(\mathbf{q})g^{zz}(\omega)G^{zz}(\mathbf{q},\omega),$$

$$G^{+-}(\mathbf{q},\omega)=g^{+-}(\omega)-\tfrac{1}{2}J(\mathbf{q})g^{+-}(\omega)G^{+-}(\mathbf{q},\omega)$$

$$(+-\leftrightarrow-+). \tag{3}$$

Hence the expression of the longitudinal mode L and the two transverse mode $T_{\pm}$ are

$$G^{zz}(\mathbf{q},\omega)=\frac{g^{zz}(\omega)}{1+J(\mathbf{q})g^{zz}(\omega)}\ (L)$$

and

$$G^{+-}(\mathbf{q},\omega)=\frac{g^{+-}(\omega)}{1+\dfrac{1}{2}J(\mathbf{q})g^{+-}(\omega)}$$

$$(T_{+}\leftrightarrow T_{-})\quad(+-\leftrightarrow-+). \tag{4}$$

As pointed out, the poles of $G^{\alpha\beta}(\mathbf{q},\omega)$ determine the spectrum of the magnetic excitations, which are then given by

$$1+J(\mathbf{q})g^{zz}(\omega)=0\quad(L),$$

$$1+\frac{1}{2}J(\mathbf{q})g^{+-}(\omega)=0\quad(T_{+}\leftrightarrow T_{-})\quad(+-\leftrightarrow-+). \tag{5}$$

In this way, for a given wave vector $\mathbf{q}_0$, and knowing the ω dependence of the single-ion susceptibilities $g^{\alpha\beta}(\omega)$ from the CEF Hamiltonian, the observation of an excitation at an energy ω_0 will allow us to deduce the corresponding $J(\mathbf{q}_0)$ value through Eqs. (5). Therefore, from the measurement of the whole dispersion curve $\omega(\mathbf{k})$ inside the Brillouin zone, one can experimentally obtain the Fourier transform of the exchange interactions and then one can make use of the inverse Fourier transform to extract the J_{ij} exchange coupling constants.

V. ANALYSIS AND DISCUSSION

The CEF parameters involved in the one-ion Hamiltonian Eq. (1) have been previously obtained[9] and constitute the starting point of the present analysis. In addition, from the magnetic measurements it was also determined that the exchange coupling constant $J(0)=-0.2$ K and $J(Q)=2.3$ K.[9] As commented in Sec. IV, the Eqs. (5) allow us to determine the Fourier transform of the intersite exchange interactions $J(q)$ whenever the CEF parameters and the dispersion curves $\omega(k)$ are known.

The theoretical values of $J(q)$ as a function of the energy transfer ω are represented in Fig. 8, and were obtained from the CEF parameters of Ref. 9 using Eqs. (5). Five excitations are expected in the experimental range 1–9 meV corresponding to the transfers: $\Gamma_2\to\Gamma_5^{(1)}$ (T); $\Gamma_1^{(1)}\to\Gamma_2$ (L); $\Gamma_1^{(1)}\to\Gamma_5^{(1)}$ (T); $\Gamma_1^{(2)}\to\Gamma_5^{(2)}$ (T); $\Gamma_2\to\Gamma_1^{(2)}$ (L). As deduced from Fig. 8, only the second and the third excitations have appreciable dispersion behavior and they are associated with the lower energy branches of Fig. 2. However, the first excitation ($\Gamma_2\to\Gamma_5^{(1)}$) has insignificant intensity, around 5% of that associated with the longitudinal $\Gamma_1^{(1)}\to\Gamma_2$ (L) excitation, and only in a few scans are there any indications of the existence of this dispersiveless branch, the energy of which is 1.8 meV. Lastly, the transverse mode referred to as the transfer $\Gamma_1^{(2)}\to\Gamma_5^{(2)}$ (T) is expected to have zero intensity at 30 K due to thermal population factors as commented before.

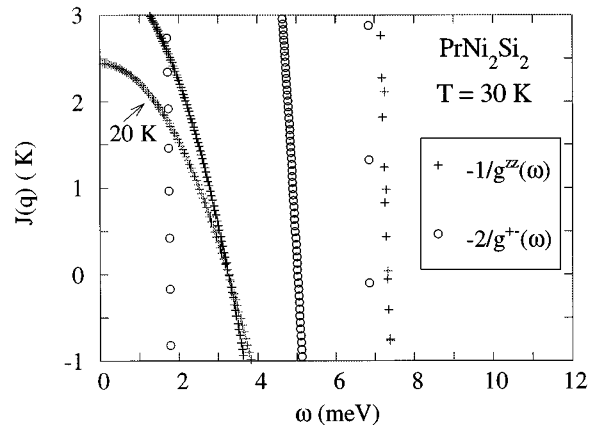

FIG. 8. Theoretical variation of $J(\mathbf{q})$ as a function of energy transfer of magnetic excitations in $PrNi_2Si_2$ at 30 K using the CEF parameters of Ref. 10 (see text). Also presented are the results for the longitudinal excitations at 20 K (g^{+-} and g^{zz} are the single-ion CEF susceptibilities, see text).

In principle, in order to account for the minimum of $\omega(k)$ at the propagation vector Q of the AM magnetic structure which appears below T_N, it is only necessary to take into account the exchange coupling constants between the two nearest neighbors. However, with this information alone, it is not possible to describe the complete dispersion curve of Fig. 2. Therefore, we need to consider the additional exchange coupling constants between more distant neighbors in order to account for all the important features observed in the lowest energy longitudinal branch.

Increasing successively the number of neighbors considered in the calculations up to the ninth nearest neighbor does not improve the fit, in particular at Q (see inset of Fig. 2). However, when the more distant neighbors of the Pr^{3+} ion along the c direction of the body-centered tetragonal structure of $PrNi_2Si_2$ are included, the results are significantly improved as is also shown in Fig. 2, where the minimum at Q is seen to be well described. This narrow minimum of the dispersion curve $\omega(k)$ around Q is associated with a sharp singularity in the electron conduction band along the c^* direction. In order to explain this feature it is necessary to consider high-order Fourier harmonics in $J(q)$. In Table I the values of exchange coupling constants J_{ij} deduced from the data are given. Because of the large number of parameters involved in the analysis of the dispersion curves, it is quite difficult to give some idea of the magnitude of the error bars in J_{ij}. However, it is worth noting that although the

TABLE I. Most important isotropic bilinear exchange coefficients J_{ij} representing the coupling with neighbor ions whose positions are defined by $r=(x,y,z)$ in $PrNi_2Si_2$. The results correspond to the cases of 8 nearest-neighbor (NN) ions along the c direction and 5 NN in the basal plane (labeled 8 NN+5 NN) and the 9 NN ions (labeled 9 NN).

	x,y,z	1 0 0	$\frac{1}{2}\,\frac{1}{2}\,\frac{1}{2}$	1 1 0	0 0 1	$\frac{1}{2}\,\frac{1}{2}\,\frac{3}{2}$	0 0 2	$\frac{1}{2}\,\frac{1}{2}\,\frac{5}{2}$	0 0 3	$\frac{1}{2}\,\frac{1}{2}\,\frac{7}{2}$	0 0 4
8 NN+5 NN	$J_{ij}(K)$	69	−181	91	142	−4	−24	18	−5	13	−56
9 NN	$J_{ij}(K)$	17	−148	101	52	−14					

exchange coupling constant J_{ij} with the first nearest neighbors (100) is positive, that with the second neighbor ($\frac{1}{2}$, $\frac{1}{2}$, $\frac{1}{2}$) is strongly negative and its magnitude is responsible for antiferromagnetic ordering in this system. Note in Fig. 2 that the parameters for the 9 NN case (see Table I) describe the general behavior in all the investigated Brillouin zone quite well, but they predict that the minimum in $\omega(k)$ must be at Z, and not at Q. This important feature which anticipates the propagation vector Q to be associated with the periodicity of the AM magnetic structure below T_N, is reproduced as commeted before, only by taking into account the more distant neighbors along the c direction. The best fit corresponds to 8 neighbors along this direction and 5 neighbors which lie in the basal plane. The magnitudes of the J_{ij} corresponding to the interaction with these latter ions are not in general large (see Table I), but they are indispensible in the calculations. By using Eqs. (5) we can represent (see Fig. 9) the shape of $J(q)$ along the main directions of the Brillouin zone which where investigated (from Eqs. (5), Figs. 2 and 9 are equivalent within the RPA). A maximum is found for the value Q corresponding to the propagation vector of the AM magnetic structure. Moreover, from this curve, the values of $J(0)=-0.5$ and $J(Q)=2.4$ K can be deduced, which are in good agreement with those determined previously from the macroscopic magnetic measurements.[9]

These J_{ij} parameters that are determined from the RPA analysis of the dispersion curves, can also be used to calculate the thermal dependence of $\omega(k)$ at the Γ, Z, and Q points. The results are presented in Fig. 6. Although there are some obvious discrepancies between theory and the experimental results concerning the absolute values corresponding

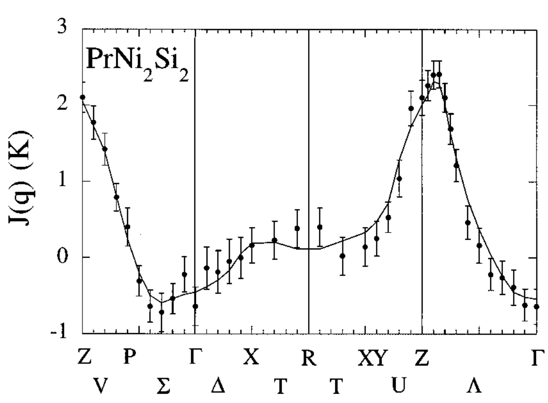

FIG. 9. The Fourier transform $J(q)$ of exchange coupling constants J_{ij} along the main directions of the Brillouin zone of the body-centered tetragonal lattice of $PrNi_2Si_2$. Solid line corresponds to the best fit using the intersite exchange parameters J_{ij} of Table I, corresponding to the case 8 NN+5 NN.

to Z and Q (the softening at the Q point between 30 and 20 K is calculate to be $\sim$85%, while experimentally we measure a softening of only 50%), the theory does correct predict that $\omega(k)$ decreases more quickly for Q than for Z when the temperature is lowered to T_N, and that the mode at Q is not a complete soft mode (see Fig. 7). This type of large dispersion in the paramagnetic excitations was also found in the nonmagnetic ground-state systems Pr metal,[12] PrSb (Ref. 13) and Pr_3T1.[11] Further investigations are needed in order to understand the change of behavior of the HWHM represented in Fig. 7 from inelastic to quasielastic type in the vicinity of T_N, in relation with critical effects.

In summary, the INS experiment performed in the singlet ground-state compound $PrNi_2Si_2$ has clearly shown the existence of several branches of well-defined excitations having different polarizations in the paramagnetic phase along the main directions of the Brillouin zone. The lowest energy branch shows a strong dispersion. This has been well accounted for quantitatively by a theory based on the generalized susceptibility formalism within the RPA, which allows us to determine the isotropic bilinear exchange interaction constants J_{ij} between Pr^{3+} ions. The analysis shows that the coupling between distant Pr^{3+} ions located along or near the c direction is required in order to stabilize the AM magnetic structure which corresponds to $PrNi_2Si_2$ below T_N. This effect is related in some way to the conduction band and the topology of the Fermi surface. Furthermore, the enhancement of $J(q)$ close to Q, as shown in Fig. 9, could be associated with this particular shape of the Fermi surface and may also be one of the reasons for the strong anomalous deviation of the de Gennes law concerning the critical temperatures of the series RNi$_2$Si$_2$,[14] which has also been observed in other RAu$_2$Si$_2$ (Ref. 15) and RCu$_2$Si$_2$ (Ref. 16) compounds. In order to account for these particular features on a more fundamental basis, band calculations are necessary. The indirect RKKY exchange interaction that can be related to the type of magnetic ordering involved is connected with the details of the Fermi surface via the generalized susceptibility $\chi(q)$ and its anomalies.

ACKNOWLEDGMENTS

The work at ORNL was supported by the U.S. Department of Energy under Contract No. DE-AC05-84OR21400 with Martin Marietta Energy Systems, Inc. Moreover, the authors would like to thank B. Fåk for his kind support in doing the inelastic neutron-scattering experiment at the ILL. One of us (J.A.) wishes to acknowledge the hospitality of the Oak Ridge National Laboratory during the experiment. Part of the work has also been partially supported by Spanish CICYT Grant No. MAT96-1023-C03.

[1] P. Bak, Phys. Rev. Lett. **46**, 791 (1981).
[2] M. H. Jensen and P. Bak, Phys. Rev. B **27**, 6853 (1983).
[3] S. W. Lovesey, J. Phys. Condens. Matter **2**, 1313 (1990).
[4] R. Currat and T. Janssen, Solid State Phys. **41**, 201 (1988).
[5] A. Szytula and J. Leciejewicz, in *Handbook on the Physics and Chemistry of Rare Earths*, edited by K. A. Gschneidner, Jr., and L. Eyring (North-Holland, Amsterdam, 1989), Vol. 12, p. 133.
[6] R. M. Nicklow and N. Wakabayashi, Phys. Rev. B **26**, 3994 (1982).
[7] C. J. Lantwin, Z. Phys. B **79**, 47 (1990).
[8] R. M. Nicklow and N. Wakabayashi, Phys. Rev. B **51**, 12 425 (1995).
[9] J. A. Blanco, D. Gignoux, and D. Schmitt, Phys. Rev. B **45**, 2529 (1992).
[10] J. A. Blanco, R. M. Nicklow, and D. Schmitt, Physica B **213&214**, 327 (1995).
[11] W. J. L. Buyers, T. M. Holder, and A. Perrault, Phys. Rev. B **11**, 266 (1975).
[12] J. G. Houman, B. D. Rainford, J. Jensen, and A. R. Mackintosh, Phys. Rev. B **20**, 1105 (1979).
[13] D. B. McWhan, C. Vettier, R. Youngbood, and G. Shirane, Phys. Rev. B **20**, 4612 (1979).
[14] J. M. Barandiaran, D. Gignoux, D. Schmitt, J. C. Gomez-Sal, and J. Rodriguez Fernandez, J. Magn. Magn. Mater. **69**, 61 (1987).
[15] I. Felner, J. Phys. Chem. Solids **36**, 1063 (1975).
[16] W. Schlabitz, J. Baumann, G. Neumann, D. Plümacher, and K. Reggentin, in *Crystalline Electric Field Effects in f-Electron Magnetism*, edited by R. P. Guertin, W. Suski, and Z. Zolnierek (Plenum, New York, 1982), p. 289.